Biophysical Chemistry 10 (1979) 161–171

POLARIZED FLUORESCENCE IN AN ELECTRIC FIELD: COMPARISON WITH OTHER ELECTROOPTICAL EFFECTS FOR RODLIKE FRAGMENTS OF DNA AND THE PROBLEM OF THE SATURATION OF THE INDUCED MOMENT IN POLYELECTROLYTES

S. SOKEROV * and G. WEILL

Centre de Recherches sur les Macromolécules C.N.R.S. and Université L. Pasteur, Strasbourg, France

Received 19 May 1978
Revised manuscript received 20 February 1979

Electrical birefringence, electrical dichroism and polarisation of fluorescence in an electric field experiments have been performed at high fields on sonicated fragments of DNA labelled with Acridine Orange. The latter electrooptical effect gives access to the field dependence of the fourth moment of the orientation function while the two former give access to the field dependence of the second moment. The origin of the large departure from an E^2 dependence at rather low degrees of orientation is extensively discussed. Following a suggestion of Shirai on the calculation of orientational averages for a saturated induced moment, we can show that this model rationalizes the existence of a linear E dependence of the orientation factor at intermediate fields and explains very well our experimental results. When applied to previous dichroic data at higher fields it shows that the low value of the dichroism at saturation introduced to fit with other models, in contradiction with the absence of base tilting in the B form of DNA, is not required for a quantitative fit with this new orientation mechanism. The transition from an E^2 dependence at low fields to an E dependence at intermediate fields gives an estimate of the field required for the saturation of the ionic polarisation $E \sim 6$ kV/cm.

1. Introduction

Electrooptical effects offer in principle several methods for the identification of the mechanism of orientation of particles in an electric field and for the measurement of their permanent dipole moment and polarizability anisotropy [1]. In the case of polyelectrolytes, the main mechanism of orientation is known to be due to the large induced moment resulting from the polarization of the counterion atmosphere [2,3,4]. In this case, the time of relaxation of the ionic polarization might be of the same order of magnitude as the rotational correlation time. The interpretation of the rise of the electrooptical effect, or its response to ac fields or reversing pulses in terms of a permanent dipole moment becomes then questionable [5]. On the other hand the high field dependence of the electric birefringence of dichroism of polyelectrolytes has often been reported to resemble that predicted for a permanent dipole moment [6], or to be a linear function of the electric field [7] in the low or intermediate degrees of orientation. An exact comparison is however very sensitive to:

i) the value of the birefringence or dichroism at saturation which cannot generally be experimentally reached. It must be deduced from structural information or extrapolated, assuming some theoretical law, to $1/E = 0$,

ii) the polydispersity of the samples,

iii) the possible role of flexibility.

One way of overcoming the last problem is to work at very low ionic strengths, where the contribution of the electrostatic repulsion to the persistence length [8,9] allows it to become much higher than the contour length of the polyelectrolyte molecule. It would, on the other hand, be very interesting to characterize the field dependence of the orientation by more than one moment. This is in principle possible from the change in the angular dependence of the light scattered

* Permanent address: Institute of Physical Chemistry, Bulgarian Academy of Science, Sofia 1040.

by large particles upon electric field orientation [10]. But for polyelectrolytes at low ionic strengths light scattering is dominated by intermolecular interactions and the method is very questionable.

It is one of the reason which led us to develop the method of polarized fluorescence in an electric field [11,12]. This new electrooptical effect depends on both the second and the fourth moment of the orientation function. We have recently performed a calculation of the fourth moment at high fields in the case of an orientation due either to a permanent dipole moment or to an anisotropy of the electrical polarizability [13].

In this paper, we use these results in a comparison of the fluorescence method with electrical birefringence and dichroism. In order to minimize the uncertainties relative to the optical factors at saturation of the orientation, the polydispersity and the flexibility, we have used as a polyelectrolyte short sonicated fragments of DNA labelled with intercalated Acridine Orange. The nucleotide to dye ratio (P/D) is taken higher than 25 to avoid energy transfer [14] and intercalation insures a unique geometry of the chromophore. Sonicated fragments with $M \sim 3 \times 10^5$ are known to have a limited polydispersity [15]. There is an increasing body of evidence that although the persistence length has the accepted values of ~600 Å at the ionic strength and concentrations used for meaningful light scattering experiments [16], it increases at ionic strength $<10^{-3}$ M and low polymer concentration [17] in such a way that fragments 700 to 1500 Å in length can be treated as rigid rods [7,18]. Theoretical estimates of the electrostatic contribution to the persistence length [8,9] support this view.

2. Basic theoretical relations

2.1. Electrical birefringence

The birefringence of a solution of rigid elongated particles at a concentration C is given by:

$$\Delta n = (2\pi/n_0)C\bar{v}(g_1 - g_2)\phi. \quad (1)$$

Here n_0 is the solvent index of refraction, $\bar{v}$ the partial molar volume of the solute, $(g_1 - g_2)$ the difference in optical polarizability per unit volume of oriented particles. The orientation factor:

$$\phi = (3\langle\cos^2\theta\rangle - 1)/2, \quad (2)$$

where θ is the angle between the electrical field E and the particle axis, is related to the second moment of the orientation function $f(\theta)$

$$\langle\cos^2\theta\rangle = \int_0^{\pi} \langle\cos^2\rangle f(\theta) \sin\theta \, d\theta \Big/ \int_0^{\pi} f(\theta) \sin\theta \, d\theta. \quad (3)$$

$f(\theta)$ is equal to $\exp(-U(\theta)/kT)$ where $U(\theta)$ is the electrostatic energy. Low field expansion of the exponential gives the classical Kerr law

$$\phi = \tfrac{1}{15} AE^2 \quad (4)$$

with $A = (\Delta\alpha/kT + \mu^2/k^2T^2)$.

$\Delta\alpha$ is the difference between the parallel and transverse polarizability and μ the permanent dipole moment of the particle. The field dependence of ϕ at higher fields has been calculated for several orientation mechanisms: permanent dipole, anisotropy of the electronic polarizability, polarization of the ionic atmosphere in the absence of counterion–counterion repulsion [20].

2.2. Electric dichroism

The change $I_0 - I = \Delta I$ in transmitted intensity in the absence and presence of an electric field, is related, to the orientation factor ϕ by

$$\log(1 + \Delta I_{\parallel}/I_{\parallel}) = -2\log(1 + \Delta I_{\perp}/I_{\perp})$$

$$= -\phi(2\cos^2\chi - 1)\log I_0/I. \quad (5)$$

χ is the angle between $\boldsymbol{\mu}_a$, the chromophore absorption transition moment, and the particle axis. The two expressions are for a parallel or a perpendicular polarization of the incident light with respect to E.

2.3. Polarized fluorescence in an electric field [12]

The four polarized components of fluorescence V_V, V_H, H_V and V_H can be expressed, in the general case, as complicated functions of $\langle\sin^2\theta\rangle$, $\langle\sin^4\theta\rangle$ and of the three angles χ, χ' and ψ which define the orientation of the absorption ($\boldsymbol{\mu}_a$) and emission ($\boldsymbol{\mu}_e$) transition moments with respect to the particle axis. For the simplest case, corresponding to the case of rigid fragments of DNA with an intercalated dye $\chi = \chi' = \pi/2$

and ψ becomes the angle between $\boldsymbol{\mu}_a$ and $\boldsymbol{\mu}_e$. The expressions reduce then to:

$$V_V \propto \tfrac{1}{8}\langle\sin^4\theta\rangle(1 + 2\cos^2\theta),$$

$$H_V = V_H \propto \tfrac{1}{4}\langle\sin^2\theta\rangle - \tfrac{1}{16}\langle\sin^4\theta\rangle(1 + 2\cos^2\psi),$$

$$H_H = \tfrac{24}{64}(1 - \langle\sin^2\theta\rangle + \langle\sin^4\theta\rangle)$$

$$+ \frac{\cos^2\psi}{64}(16 - 16\langle\sin^2\theta\rangle - 2\langle\sin^4\theta\rangle). \quad (6)$$

One sees that $\Delta V_V/V_V$, the relative change of V_V upon orientation is independent of ψ and defines a new orientation factor Δ

$$\Delta = 1 - \tfrac{15}{8}\langle\sin^4\theta\rangle = \Delta V_V/V_V. \quad (7)$$

At low fields

$$\Delta = \tfrac{2}{21}AE^2 \quad (8)$$

and we have calculated this quantity at high fields for an orientation by a permanent dipole moment or by an anisotropy of the electrical polarizability [13].

One sees from relation (6) that for $\chi = \chi'$ the relative change in the other components does not give additional information. It can be numerically calculated with the values of $\langle\sin^2\theta\rangle$ and $\langle\sin^4\theta\rangle$ derived from ϕ and Δ, and the value of ψ obtained from the fluorescence anisotropy r in the absence of electric field:

$$r = \frac{V_V - H_V}{V_V + 2H_V} = \frac{3\cos^2\psi - 1}{5}. \quad (9)$$

Their measurements provide however a check of internal consistency, and in particular the verification of the relation

$$(\Delta H_V - \Delta V_H) = (\Delta H_H + 2\Delta H_V) = -(\Delta H_H + 2\Delta V_H)$$

$$\propto (\cos^2\chi - \cos^2\chi') \sim 0 \quad (10)$$

This expression is strictly valid at low fields [12] but remains verified [13] for intermediate degrees of orientation.

3. Experimental procedures

3.1. Rodlike fragments of DNA

Calf thymus DNA has been sonicated at a concentration of ~0.1 gr/ℓ in 0.1 M NaCl for times ranging from 2′ to 6′ in a Mullard 3100 instrument operating at 20 kHz at a power of ~30 W. The solutions have then been dialyzed against water and kept at low temperatures. The addition of AO and the final concentration have been controlled by optical density measurements. The electrooptical experiments have been performed at a concentration between 3 and 11×10^{-4} M in nucleotide, high enough to avoid thermal denaturation at room temperature in the absence of added salt, as shown by an optical density versus temperature melting profile.

Owing to our previous experience on the molecular weight and size of sonicated fragments [18] their characterization has been limited to the measurement of the rotatory diffusion constant from the initial slope of the field free decay of the birefringence at low field.

3.2. Optical measurements

3.2.1. Birefringence

Kerr effect measurements have been performed with a simple apparatus built from a He-Ne 2 mW laser, two Glazebrook prisms and a Radiotechnique photomultiplier. The principle of quadratic detection involves the calibration of the phase difference due to birefringence by comparison with the angle of rotation of the analyzer required to obtain the same intensity. It is important, when working in a large range of birefringence to limit the intensity and to spread the emerging beam on the photocathode. This is achieved by interposition of a polaroid film at an angle before the polarizer and of a divergent lens after the analyzer. The charging resistor of the photomultiplier was sufficiently low (10 kΩ) to make the intrinsic decay time of the order of 1 μs as seen in a calibration test using nitrobenzene. This value is small enough to not influence the measurement of the rotational correlation time of DNA fragments.

3.2.2. Linear dichroism and fluorescence measurements

These experiments have been performed on a T-jump instrument with both absorption and fluorescence detection, as described previously [12]. The instrument has been equipped with Polaroid polarizers. Linear dichroism measurements require an high enough optical density (~1) to reach sufficient accuracy while fluorescence measurements require a lower optical density (~0.1 to ~0.2) to minimize the correction due to the

Table 1
Molecular and electro-optical parameters, according to the different interpretation schemes, of sonicated DNA

	Sonication time		
	2'	4'	6'
Rotational diffusion constant D (s^{-1})	4850	7300	9100
Length L (Å)	1470	1200	1100
Polarizability anisotropy $\Delta\alpha$ (cm^3)	4.6×10^{-16}	3.5×10^{-16}	2.15×10^{-16}
Permanent dipole moment μ (Debyes)	5000	3800	2300
Saturated induced moment μ_∞ (Debyes)	2300	2600	2000

effect of the linear dichroism on the screening of the incident intensity I_0 by the layers placed before the observed fluorescent volume. We have discussed previously this instrumental effect and proposed [12] a first order correction:

$$(\Delta V_V/V_V)_{corr} = \Delta V_V/V_V - \tfrac{1}{2}\Delta V_\parallel/I_\parallel,$$

$$(\Delta H_V/H_V)_{corr} = \Delta H_V/H_V - \tfrac{1}{2}\Delta I_\parallel/I_\parallel,$$

$$(\Delta V_H/V_H)_{corr} = \Delta V_H/V_H - \tfrac{1}{2}\Delta I_\perp/I_\perp,$$

$$(\Delta H_H/H_H)_{corr} = \Delta H_H/H_H - \tfrac{1}{2}\Delta I_\perp/I_\perp. \qquad (11)$$

Linear dichroism experiments have been performed at $\lambda = 490$ nm, corresponding to the maximum of the A.O absorption. Fluorescence experiments have been performed at an excitation wave length $\lambda = 436$ nm, corresponding to a strong line of the xenon-mercury lamp, with a Wratten 16 filter to eliminate the scattered light on the fluorescent beam. Linear dichroism measured at this latter wave lengths is used in relation (11). With this choice of wave lengths, the same solution can be used for both types of measurements.

3.2.3. Cell, electrodes and pulse generatore

A simple selected square spectrofluorometric suprasil cell (Hellma) was found to have a sufficiently low residual birefringence to be used in all experiments. Stainless steel horizontal electrodes, kept at a precisely measured distance by a special Teflon holder have been designed. In order to obtain large enough electric pulses a simple generator derived from the designs of Griffing [21] and Glick [22] has been built. The discharge of a 10 μF capacitor is monitored through the cell or directly to the earth by two high voltage SKT 16 Semimikron solid state thyristors. They are successively triggered by the front and the end of a square pulse. Considering the resistance of the cell in normal conditions (1 cm^2 electrodes 1.5 mm apart in 10^{-4}–10^{-3} M solutions) pulses of 500 μs can be obtained with a voltage decay smaller than 5%. The pulse voltage was measured across a calibrated resistor in parallel with the cell and displayed on a dual beam recording oscilloscope, together with the optical signal. A picture of the screen is taken for amplitude and decay measurements. For low field measurements the cell was inserted in a bridge allowing for a five fold voltage reduction.

4. Experimental results

Three samples, sonicated for 2', 4' and 6' have been used. Their rotatory diffusion constants and length according to Broersma formula [23] are given in table 1. A log plot of the field free decay of birefringence for the 4' sample is given in fig. 1. No significant change of the relaxation behaviour and initial relaxation time has been found when operating at higher field.

The variations of the transmitted intensity in the linear dichroism experiments and of the component V_V

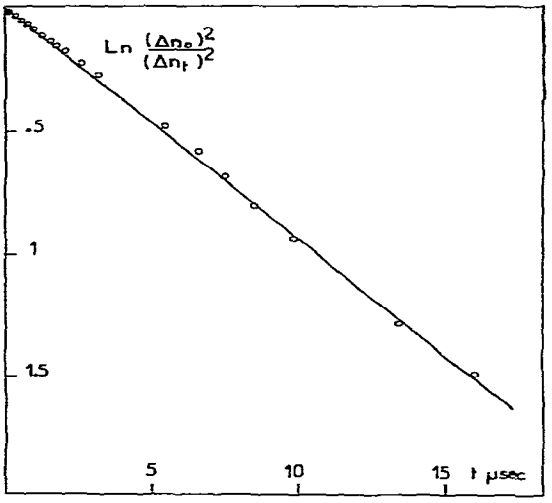

Fig. 1. Field free decay of birefringence of the 4' sample.

in the fluorescence experiment have been treated according to relations (5), (7) and (11). The orientation factors ϕ and Δ have been plotted as a function of E^2 in figs. 2, 3 and 4. They present a very large departure from a linear dependence for values higher than 0.1. Electric birefringence data can be matched to the linear dichroism data by a proper choice of $g_1 - g_2$ in relation (1). Values of ϕ derived from relation (1) with $\bar{v} = 0.53$ and $g_1 - g_2 = 21.5 \times 10^{-3}$ are plotted in the same figures.

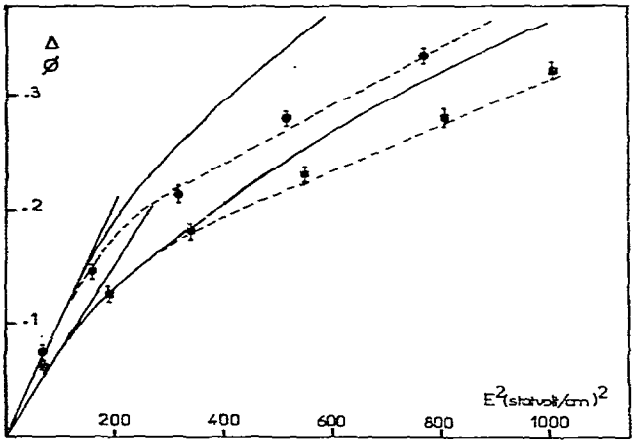

Fig. 2. E^2 field dependence of the orientation factors ϕ (from birefringence □ and dichroism ■) and Δ (from fluorescence ●) — 2' sonicated DNA. The full curve are calculated for a permanent dipole moment μ calculated from the low field linear part. The dotted curve is calculated for a distribution of electrical anisotropies (see text and table 2).

The relative changes of the polarized components V_H, H_V and H_H have only been measured in detail for the 4' sample. They are plotted after correction according to relation (11) on fig. 5. At high fields the correction becomes of the order of 25%. It is however seen that relation (10) with $\chi = \chi'$ holds showing the consistency of the corrected results. The value of the anisotropy of fluorescence $r = 0.19$, corresponding to

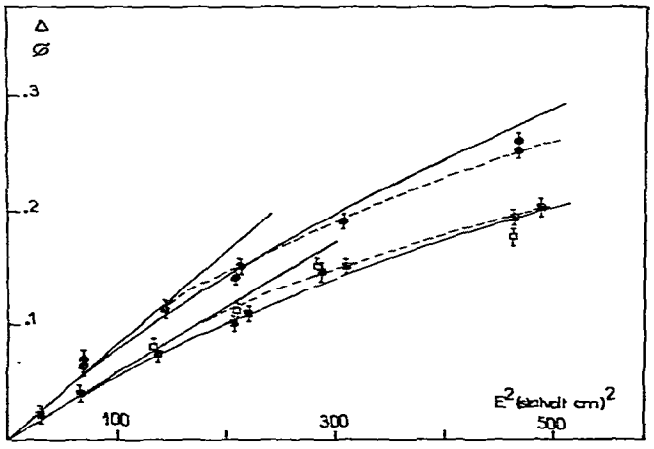

Fig. 3. ϕ and Δ for the 4' sonicated DNA — see fig. 2.

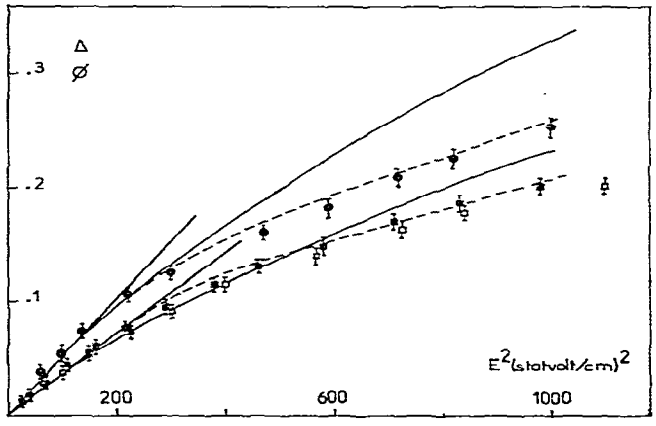

Fig. 4. ϕ and Δ for the 6' sonicated DNA — see fig. 3.

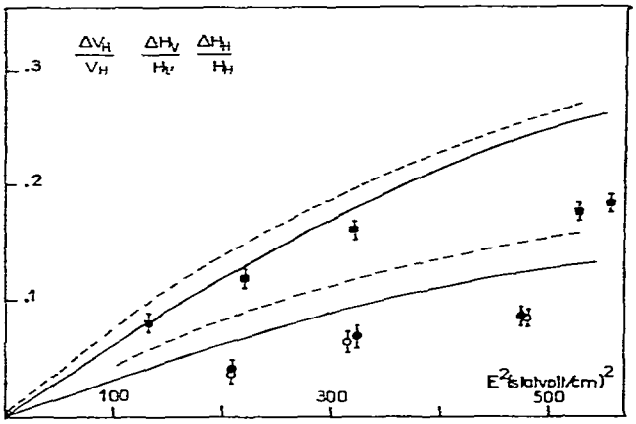

Fig. 5. Field dependence of the relative changes in the polarized components of fluorescence V_H ○, H_V ● and H_H ■ (4' sonicated DNA).

$\cos^2\psi = 0.65$, has been calculated from the absolute values of the fluorescence components V_V and H_V in the absence of electric field. These values have to be corrected for the difference in transmission and sensitivity of detection with the polarization of the fluorescent beam. For that purpose one takes advantage of the symmetry relation $H_V = V_H = H_H$ in the absence of orientation.

5. Discussion

5.1. Classical models

Relations (4) and (8) indicate that the initial tangents in the E^2 dependence of ϕ and Δ should be in a ratio 0.7. This prediction, which has already been verified in previous works [11,12], is compatible with the experimental results of figs. 2, 3 and 4. The corresponding values of A, expressed in terms of polarizability anisotropy $\Delta\alpha$ or in terms of pure permanent dipole moment μ are given in table 1.

As the theoretical dependence of ϕ and Δ for an anisotropic polarisability mechanism of orientation, is essentially linear in E^2 up to values ~0.5, the pronounced downward curvature at much lower values seen in figs. 2, 3 and 4 indicate an essential failure of this model.

Since theory predicts such a curvature for a permanent dipole mechanism of orientation we have calculated the field dependence of ϕ and Δ using the value of ϕ deduced from the initial tangent. There is a priori not much physical ground for a true permanent electric dipole, considering the antiparallel double helical structure of DNA, but the model has nevertheless already been used [6]. The calculated curves, using tabulated values of ϕ and Δ as a function of $\mu E/kT$ [13,18], have been drawn as full lines on figs. 2, 3 and 4. They reproduce the initial curvature but present an increasing departure from experiment at higher field, the measured values being always lower than the calculated ones especially for $E^2 > 500$ CGS.

A better fit to the field dependence predicted for a permanent dipole model could be obtained by modifying the value of the dichroism at saturation, as already made by some authors. The required change would however destroy the agreement between ϕ and Δ at low fields.

As the agreement between theoretical and calculated values of ϕ and Δ is nearly quantitative for the 4' sample with $E^2 < 500$ CGS (fig. 3) we have recalculated the field dependence of $\Delta H_H/H_H$ and $\Delta H_V/H_V$. As relation (6) indicates, these components depend upon differences between $\langle\sin^2\theta\rangle$ and $\langle\sin^4\theta\rangle$ and must be very sensitive to the details of the orientation mechanism. As shown in fig. 5, the agreement is not very good.

5.2. Possible polydispersity effects

Starting from the structural inconsistency of a permanent dipole moment, Houssier [26] has proposed, in his interpretations of the electric birefringence and dichroism of DNA and nucleoproteins, to fit the field dependence of ϕ with the weighted sum of orientation factors corresponding to different values of the anisotropy of electrical polarisability.

$$\phi = \sum w_i \phi(\Delta\alpha_i), \qquad \sum w_i = 1. \tag{12}$$

From a numerical point a view it is obvious that such a procedure is able to explain any curvature, the high polarizability terms reaching saturation when the low polarizability terms have still an E^2 dependence. From a physical point of view such a sum should be justified by some type of polydispersity.

Assuming a similar shape for Δ

Table 2
Fitting of the field dependence of ϕ and Δ with a sum of anisotropic polarizabilities: relative weights and anisotropies

	Sample		
	2'	4'	6'
w_i, $\Delta\alpha_i$ (cm^3)	85% 1.20×10^{-16}	70% 1.06×10^{-16}	90% 0.75×10^{-16}
w_i, $\Delta\alpha_i$ (cm^3)	15% 24×10^{-16}	20% 3.2×10^{-16}	10% 15×10^{-16}
		10% 21.2×10^{-16}	

$$\Delta = \sum w_i \Delta(\Delta\alpha_i), \qquad (13)$$

we have fitted our curves with a unique set of two or three w_i and $\Delta\alpha_i$ for both orientation factors. For the three samples a very satisfactory agreement can be reached, as shown by the dotted lines in figs. 2, 3 and 4. The required values of w_i and $\Delta\alpha_i$ are given in table 2. Considering the difference in the extreme values of $\Delta\alpha_i$, it should also be reflected in the field free decay.

If we attribute it to the polydispersity in length, and since the ionic polarization of rigid polyelectrolytes is believed to be proportional to L^3, as is the rotational correlation time τ, there should be:

i) Large discrepancies in the average length as deduced from the weight average molecular weight (obtained by light scattering at higher ionic strength and the mass per unit length of the Crick and Watson structure) and from the field free decay of birefringence at low fields which is the cubic root of the product of the weight, z and $z + 1$ averages [25]). We have never observed such discrepancies for sonicated fragments [17].

ii) A large change in the field free decay with the degree of orientation, with the progressive apparition of faster components of increasing amplitude. We have not observed such changes in our experiments. Houssier [26] reports a change in mean relaxation time for a sonicated sample of molecular weight $\sim 5 \times 10^5$ from 40 μs at $E \sim 1$–2 kV/cm to 20 μs at $E > 6$ kV/cm. The detailed comparison of his results [24] for the distribution of $\Delta\alpha_i$ (from the field dependence of ϕ) and of τ_i (from the field free decay near saturation) reveals in this case a much broader distribution for $\Delta\alpha_i$ than for τ_i.

Houssier, without discussing this latter point, qualitatively invokes the model of a kinked chain of rigid rods, developed by Van der Touw and Mandel [27] for the interpretation of the dielectric dispersion of polyelectrolytes solutions, to justify the relation (12) as originating from the chain flexibility. This is not very clear to us. In this model, the kinking is time independent and introduces a potential bareer between segmental and overall fluctuations of the counterion distribution. There are therefore two time constants for the redistribution of the counterions in the presence of the field and two regions of dielectric dispersion, the low one being molecular weight dependent.

However, since the model has a time independent conformation, there is only one rotational correlation time and one, frequency dependent, polarizability anisotropy associated with each chain. For molecules of identical molecular weight a distribution of polarizabilities could only arise from a fluctuation in the length of the subunits or of the potential barrier associated with the kinks. This could probably broaden the distribution of anisotropies compared to the dis-

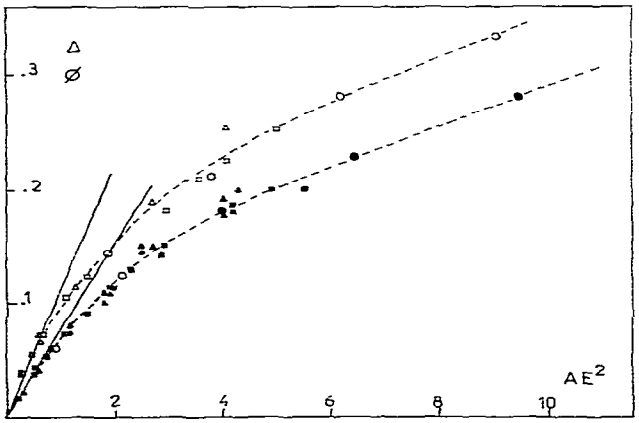

Fig. 6. E^2 field dependence of ϕ and Δ normalized to the initial slope $AE^2/15$ for the three samples (2' sonicated •○, 4' sonicated ▲△, 6' sonicated ■□.

tribution of rotational correlation times. But such an heterogeneity should be largely averaged out if one takes in account the time dependence of the kinking at the time scale of an electrooptical measurement (~0.6 ms). Moreover it should be remembered that:

i) there is no indication for a large flexibility of our DNA fragments at low ionic strengths [18].

ii) other interpretations of the dielectric dispersion of polyelectrolytes have been proposed [28].

Another indication for the lack of a large polydispersity in our samples come from the plot of all our results in a single representation as shown in fig. 6. ϕ and Δ are plotted for each sample against AE^2, where $A/15$ is the initial slope of ϕ for the considered sample. It is seen that all our points define a unique master curve for ϕ and Δ. It implies that the strong downward curvature must reflect a true and new mechanism of orientation.

5.3. Saturation of the induced moment

Faced with similar findings in his study of the electrical birefringence of polystyrene sulfonate (where chain flexibility may be higher and the birefringence at saturation is unknown, so that absolute values of ϕ cannot be obtained) Yoshioka [29] has suggested that the curvature should be attributed to the progressive saturation of the ionic polarization. Indeed the full development of the original Mandel's model by Neuman and Katchalsky [30] leads to an expression of the induced moment

$$\mu_{\text{ind}} = \frac{nzeL}{2}\left[\coth\frac{zeLE}{2kT} - \frac{1}{N}\coth\frac{zeLE}{2NkT}\right], \qquad (14)$$

with a limiting value $\mu_\infty = nzeL/2$. Here L is the polyelectrolyte length, N the number of its ionic sites, n the number of mobile counterions of valency z in the ionic atmosphere. A non linear dependence of μ_{ind} is expected for $\mu_{\text{ind}} > \mu_\infty/2$. This corresponds, for DNA fragments with $L = 1200$ Å and $N = 700$, to $E = 25$ CGS i.e. 7500 V/cm.

Yoshioka [20] has given the expression of the field dependence of ϕ for such a model

$$\phi = \left\{3\int_0^1 u^2\frac{\sinh(\kappa u)^n}{\kappa u}\,du \Big/ 2\int_0^1 \frac{\sinh(\kappa u)^n}{\kappa u}\,du - \frac{1}{2}\right\}, \qquad (15)$$

where $u = \cos\theta$ and $\kappa = zeLE/2kT$ and carried out numerical calculations for different values of n. We have done the same for Δ but we shall not insist on that, since the following examination of ϕ alone shows the inadequacy of these expressions.

In the limit of low K, one recovers the classical expression

$$\phi = \tfrac{1}{15} n z^2e^2L^2/12k^2T^2 \qquad (16)$$

corresponding to an anisotropy of polarizability

$$\Delta\alpha = n z^2e^2L^2/12kT$$

or formally to a permanent dipole moment

$$\mu = (n/12)^{1/2}zeL.$$

If nL is large the saturation of orientation will take place before the saturation of the polarization. For the reverse to hold one must have very small values of $n \sim 1$. Then the field dependence of ϕ resembles very much that for a permanent dipole moment $\mu = \mu_\infty$.

From the values of $\Delta\alpha$ given in table 1, one calculates values of n between 3.5 and 5 for the three samples, as compared to values of N between 650 and 860. This two order of magnitudes difference has already been stressed and interpreted as resulting from counterion–counterion repulsion [3,31].

With such values of n, the variation of ϕ would roughly correspond to that due to a permanent dipole moment, the value of which increases with the field from $(n/12)^{1/2}zeL$ to $(n/2)zeL$. It can never be lower than that calculated for a permanent dipole moment $(n/12)^{1/2}zeL$.

Shirai [32] has developed another model for the saturation of the induced moment. It suffers the same weakness not to take in account counterion–counterion repulsion, leads to results very similar to those of Yoshioka in the extreme cases, but contain a very interesting remark. Shirai points out the fact that in the calculation of the average from relation (3) one should very carefully distinguish between a permanent dipole moment or a saturated induced dipole moment. Indeed in the latter case the electrostatic energy for the two orientations θ and $\pi - \theta$ is equal and the integration should therefore be performed between 0 and $\pi/2$. Therefore

$$\langle\cos^n\theta\rangle = \int_0^{\pi/2}\cos^n\theta\,\exp\{(\mu_\infty E/kT)\cos\theta\}\sin\theta\,d\theta \times\left[\int_0^{\pi/2}\exp\{(\mu E/kT)\cos\theta\}\sin\theta\,d\theta\right]^{-1}. \qquad (17)$$

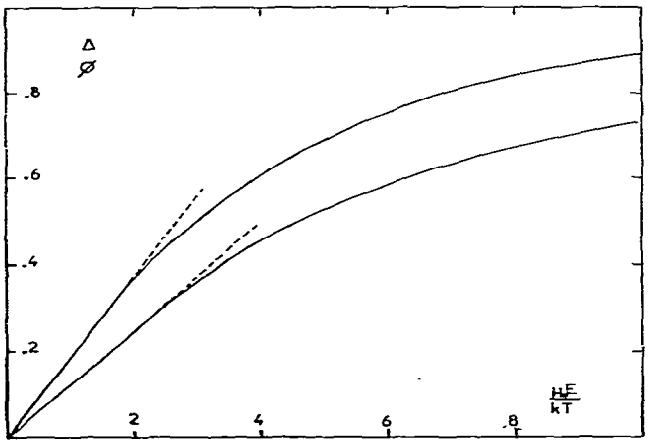

Fig. 7. Theoretical field dependence of ϕ and Δ for the model with a saturated dipole moment μ_∞.

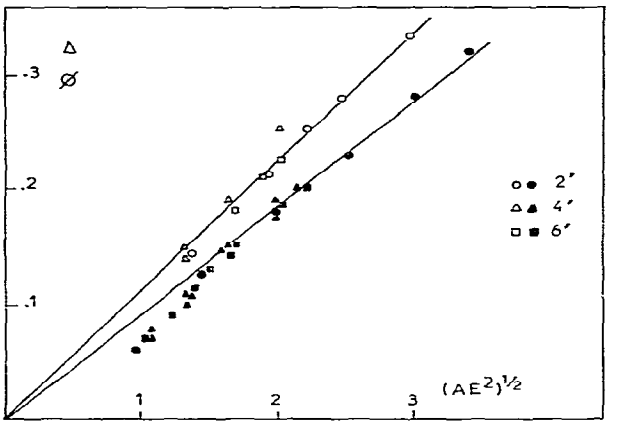

Fig. 8. Data of fig. 6 plotted as a function $A^{1/2}E$.

If the saturation of polarization is reached at values of E sufficiently low so that $\mu_\infty E \ll kT$ we can develop the exponential and realize that the term linear in E does not vanish.

One finds easily the integrals involved in relation (17)

$$\int x^n e^{ax} dx = (e^{ax}/a^{n+1})[ax^n - n(ax)^{n-1} + n(n-1)(ax)^{n-2} + (-1)^{n-1} n!(ax) + (-1)^n n!].$$

We have used them to calculate the field dependence of ϕ and Δ as given in fig. 7. The linear field dependence corresponding to the low field expansion

$$\phi = \tfrac{1}{8}\mu_\infty E/kT, \qquad \Delta = \tfrac{3}{16}\mu_\infty E/kT,$$

$$\mu E/kT \ll 1 \tag{18}$$

is in fact valid up to $\mu E/kT \sim 3$. At larger field, one finds as expected, the same expansion as for a true permanent moment

$$\phi = 1 - 3\frac{kT}{\mu_\infty E} + 3\left(\frac{kT}{\mu_\infty E}\right)^2 \qquad \Delta = 1 - 15\left(\frac{kT}{\mu_\infty E}\right)^2$$

$$\mu E/kT \to \infty. \tag{19}$$

We have therefore replotted in fig. 8 the data of fig. 6 as a function of $(AE)^{1/2}$. There is obviously a transition from an upward curvature representative of a low field E^2 dependence to a linear dependence at intermediate field. The slopes of the linear part of ϕ and Δ are in a ratio of 0.8 as compared to the value of 0.66 expected from relation (18). This could be due to the fact that the induced moment is still slowly varying in that field range. Replotting separately the results of figs. 2, 3 and 4 we can calculate from the slope of ϕ versus E, the values of μ_∞ given in table 1. We can also evaluate from the transition between the E^2 and the E dependence a value of the field required to saturate the ionic polarization $E \sim 6$ kV/cm.

Since our results are limited to values of $\phi < 0.3$, where no high field deviation from a linear E dependence is expected, as seen in fig. 7, we have looked for further support to the model by reconsidering the results of other authors, on the high field electric dichroism of DNA fragments.

5.4. Reinterpretation of previously published high field dichroism data

We shall first consider the most recent work by Hogan, Dattagupta and Crothers [7]. They have studied short monodisperse fragments of DNA from nuclease digested chromatine with 230 base pairs and a length ~780 Å. They report a linear E^2 dependence of the electric dichroism in the low field region up to 6 kV/cm. In order to interpret their data, they:

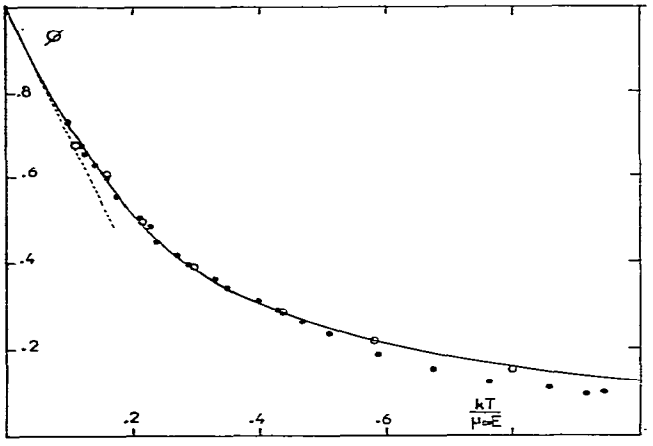

Fig. 9. Theoretical field dependence of ϕ and Δ for the model with a saturated dipole moment ϕ_∞. Plot as a function of $(\mu E/kT)^{-1}$ for high field data. Experimental points are from ref. [6] • and [7] ○.

i) develop a rather artificial model with an orientation energy of the type $U = -AE\cos^2\theta$, an "ad hoc" assumption to get a linear term in E from the low field expansion of relation (3) with the "normal" limits of integration,

ii) calculate their fit using a value of the dichroism at saturation, obtained from a linear $1/E$ extrapolation, which corresponds to a base tilting with $\chi = 75°$ $(1 - 3\cos^2\chi = 0.80)$.

Their results can be most satisfactorily accounted with the field dependence of fig. 7, assuming a negligible base tilting $(1 - 3\cos^2\chi = 0.965, \chi = 84°)$ and $\mu_\infty = 6800$ D, as clearly shown in fig. 9, where the theoretical dependence of ϕ as a function of $(\mu E/kT)^{-1}$ has been plotted together with their reinterpreted values. It is instructive to see the error on the limiting dichroism which can arise when using a linear E^{-1} extrapolation from values of $\phi < 0.70$.

For that reason we have also replotted in fig. 9 the data of Ding, Rill and Van Holde [6] for their 7.2 s sonicated sample, $L \sim 1600$ Å. We used the same limiting dichroism in place of the value they chose to get a best fit for a classical permanent dipole moment mechanism of orientation $(1 - 3\cos^2\chi = 0.90, \chi \sim 80°)$. The agreement is now very good with $\mu_\infty = 6000$ Debyes. The low field deviation, similar to that in our experiments, indicates that saturation takes place around $E = 6$ kV/cm.

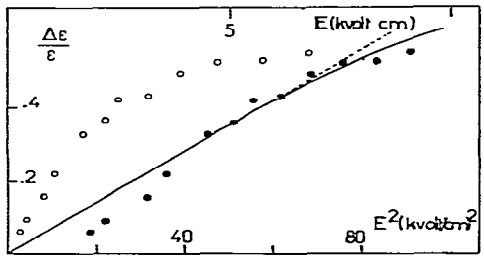

Fig. 10. A plot of the electric dichroism data of ref. [33] as a function of E^2 and E. The curve is calculated for a saturated induced moment.

The intermediate field data of Charney and Yamaoka [33], who from an E^2 plot of the dichroism of a sonicated DNA, $L \sim 1200$ Å, suggested a limiting dichroism as low as 0.6, have been replotted in fig. 10 as a function of E. Once again, it is seen that our interpretation gives a much more reasonable fitting of the experimental data with $\mu_\infty \sim 5200$ D.

Considering the values of μ_∞ obtained for different short DNA there still seems to be rather large discrepancies which could very well arise from differences in concentration and ionic strength. Indeed, our dichroic experiments in the visible with an intercalated dye require concentrations ~10 times larger than those used when studying the intrinsic dichroism of the bases in the UV region. Also important is the problem of field homogeneity when using directly the electrodes of a T-jump cell [7]. This point deserves further clarification considering the highest value derived for the shortest DNA.

Since electric birefringence might be the easiest and most accurate way for further investigation in a large range of experimental conditions, a precise knowledge of the optical anisotropy factor $(g_1 - g_2)$ is of great interest. The consistance of the dichroic data in the base or intercalated dye absorption bands, with $\chi \sim 90°$ gives confidence into the value that we have derived when comparing birefringence and dichroic data $g_1 - g_2 = 21.5 \times 10^{-3}$. This value is in good agreement with that found by Houssier [24]. It differs however very much from the value precedently given by one of us [18] where it was calculated from a comparison of flow and electric birefringence. In this case the calculation makes use of the value of the rotatory diffusion constant D obtained by flow birefringence which is very sensitive to polydispersity.

6. Conclusion

The development of correct expressions, based on a remark of Shirai, for the orientation due to a saturated induced dipole moment, leads to a very satisfactory interpretation of our results as well as previously published data. This gives a strong support to the idea of a low field (~6 kV/cm) saturation of the ionic polarization in DNA. New experiments, using birefringence, dichroism and fluorescence on monodisperse fragments are now required for a quantitative discussion of the relation between the saturated moment, the onset of saturation, and the polymer length, charge, and concentration at different ionic strengths and with different counterions.

Acknowledgements

This work was performed during a stay of S. Sokerov in Strasbourg made possible by a grant from the French Government and the help of Professor H. Benoit. Thanks are due to J.P. Beyl for building the pulse generator, to G. Duportail for his help in obtaining sonicated fragments of DNA and J.J. André for programming some of the numerical calculations. Pr. Shirai has kindly provided us with a copy of unpublished theoretical results which have played a major role in the interpretation of our experiments.

References

[1] See for example
R. Fredericq and C. Houssier, Electric dichroism and electric birefringence (Clarendon Press Oxford, 1973);
Molecular electrooptics, ed. C.T. O'Konski (M. Dekker N.Y., 1977);
S.P. Stoylov, Adv. Colloid Interface Sc. 3 (1971) 45;
B.R. Jennings, Adv. in Mol. Relax. Processes 10 (1977) 15.
[2] H. Schwarz, Physik Chem. Neue Folge 19 (1959) 286.
[3] M. Mandel, Mol. Phys. 4 (1960) 489.
[4] F. Oosawa, Biopol. 9 (1970) 677.
[5] Light Kuangchung Sun, Ph. D. Dissertation, University of New Mexico, Albuquerque 1976.
[6] D.W. Ding, R. Rill and K.E. Van Holde, Biopol. 111 (1972) 2109.
[7] M. Hogan, N. Dattagupta and D.M. Crothers, Proc. Natl. Ac. Sc. 76 (1978) 195.
[8] T. Odijk, J. Pol. Sc. 15 (1977) 477.
[9] T. Skolnick and M. Fixman, Macromolecules 10 (1977) 944.
[10] M.V. Stoimenova, J. Coll. Interface Sc. 53 (1975) 42.
[11] G. Weill and C. Hornick, Biopol. 10 (1971) 2029.
[12] G. Weill and J. Sturm, Biopol. 14 (1975) 2537.
[13] S. Sokerov and G. Weill, Biophys. Chem. 10 (1979) 41.
[14] G. Weill and M. Calvin, Biopol. 1 (1963) 401.
[15] G. Cohen and H. Eisenberg, Biopol. 4 (1966) 429.
[16] D. Jolly and H. Eisenberg, Biopol. 15 (1976) 61.
[17] R.E. Harrington, Biopol. 17 (1978) 919.
[18] G. Weill, C. Hornick and S. Stoylov, J. Chem. Phys. 65 (1968) 182.
[19] C.T. O'Konski, K. Yoshioka and W.H. Orttung, J. Phys. Chem. 63 (1959) 1558.
[20] K. Kikuchi and K. Yoshioka, Biopol. 15 (1976) 583.
[21] R. Griffing, Rev. Sc. Instr. 45 (1976) 964.
[22] H.A. Glick, Rev. Sc. Instr. 47 (1976) 150.
[23] S. Broersma, J. Chem. Phys. 32 (1960) 1626.
[24] C. Houssier, Thèse d'aggregation, Liège 1977.
[25] J. Coles and G. Weill, Polymer 18 (1977) 1235.
[26] C. Houssier, J. Bontemps, Xavier Edmonds-Alt and E. Fredericq, Annals of N.Y. Ac. Sc. 303 (1977) 107.
[27] F. van der Touw and M. Mandel, Biophys. Chem. 2 (1974) 218.
[28] A. Minakata, Annals of N.Y. Ac. Sc. 303 (1977) 107.
[29] K. Kikuchi and K. Yoshioka, J. Phys. Chem. 77 (1973) 2101.
[30] E. Neumann and A. Katchalski, Proc. Nat. Ac. Sc. 69 (1972) 993.
[31] G. Weill and C. Hornick, in: Polyelectrolytes, ed. E. Selegny (Reidel Pub. Co, Dordrecht, 1974) p. 277.
[32] M. Shirai, Field dependence of the electric birefringence of polyelectrolyte solutions - preprint.
[33] E. Charney and K. Yamaoka, Macromolecular Preprints (1971) vol. 1.